

Density and temperature effects on electron mobility in fluid methane

Norman Gee and Gordon R. Freeman

Chemistry Department, University of Alberta, Edmonton, Alberta T6G 2G2, Canada

(Received 8 December 1978)

The mobility μ electrons in methane at $n < 6 \times 10^{20}$ molecule/cm³ is field dependent at $E/n > 0.012$ Td ($1 \text{ Td} = 1 \times 10^{-17} \text{ Vcm}^2/\text{molecule}$). The temperature dependence of the thermal-electron mobility in the low-density vapor is $\mu n \propto T^{0.45}$. The threshold field and temperature dependence are much lower than reported previously. In the electron energy region $0.002 < \epsilon < 0.2$ eV the momentum-transfer cross section of methane molecules is well approximated by $\sigma_v = 0.014v^{-1.9} \text{ cm}^2$. In the low-density gas the electron drift velocity v_d becomes superlinear with field strength at threshold velocity $v_d^{\text{thr}} = c_0$, the speed of low-frequency sound. At $n > 6 \times 10^{20}$ the value of μn in the coexistence gas decreases slightly, while $d(\mu n)/dT$, $(E/n)_{\text{thr}}$, and v_d^{thr}/c_0 increase. The effects are due to quasilocation of the electrons by density fluctuations in the dense gas. The entropy $\Delta S'$ and enthalpy $\Delta H'$ of activation of electron transport correlate with the structure factor $S(0)$ of the dense gas: $\Delta S'/S(0) = 19 \text{ J/molK}$ and $\Delta H' \approx T\Delta S'$ near the vapor-liquid coexistence region. At $n > 6 \times 10^{21}$ there is a rapid increase in μn due to conduction-band formation. $(E/n)_{\text{thr}}$ passes through a cusp > 0.04 Td at $n = 8 \times 10^{21}$, where $d\mu/dE$ changes sign, then decreases again to 0.01 Td at $n > 1.0 \times 10^{22}$ molecule/cm³. The threshold E/n in the normal liquid is similar to that in the low-density gas. At low field strengths the electron energy is moderated mainly by elastic collisions in the low-density gas, and by inelastic collisions in the liquid.

I. INTRODUCTION

The mobility of electrons in the heavy noble liquids is characterized by a density dependence that displays a maximum.¹⁻³ Similar behavior occurs in certain liquid hydrocarbons.⁴⁻⁸ The maximum is less pronounced when the molecular shape is less spherelike.⁶

The mobility of electrons in liquid methane is similar to that in argon.⁹ The behavior in methane is interesting on the one hand because methane is the simplest, most spherelike hydrocarbon, and on the other because it is a polyatomic molecule, whereas the similarly behaving argon molecule is monatomic.

The electron scattering cross section of low-density gas-phase methane was measured nearly a half century ago.¹⁰ A plot of cross section against electron energy displays a deep minimum at ~ 0.5 eV,^{10a} compared to ~ 0.3 eV in argon and ~ 0.6 eV in krypton.^{10b} The mobility maximum at a certain density in the liquid seems to be related to the minimum in the gas-phase scattering cross section at a certain electron energy.^{11,12}

Measurements in methane have now been extended over wide ranges of density and temperature, from the low-density gas through the critical region to the normal liquid. A report of zero-field mobilities of excess electrons in dense methane gas has appeared recently.¹³

II. EXPERIMENT

A. Materials

The methane was either Matheson Research Purity (99.99%) or Linde Ultra High Purity (99.97%). The cylinder was fitted to a grease-free vacuum rack through a Pyrex Kovar seal welded to a flexible stainless-steel tube. The gas was passed through freshly activated Molecular Sieves 3A in a trap at 195 K, and condensed in a bulb at 77 K. The sample was degassed, then transferred to a freshly generated potassium mirror. An isopentane slush (113 K) maintained the methane in the liquid phase to facilitate purification by the mirror. The 50-cm³ sample was treated with seven fresh mirrors for 8 h each. The mirrors were regenerated under vacuum.

B. Equipment

The conductance cells were similar to the thick-walled cells described in Ref. 6. The one used for gas-phase measurements had side arms rotated 180° vertically compared to that in Figure 1 of Ref. 6. When in use, the liquid reservoir remained below the electrodes. Prior to filling, the cell was degassed by heating to 200 °C while evacuating to 0.1 mPa. The body of the cell was coated on the outside with Aqua Dag (GC Electronics TV Tube Coat), except for the high-voltage side arm and a 1-cm-wide strip around it. The

high-voltage arm was wrapped in Teflon tape to increase insulation. The electrode gap was 3.2 mm and the effective collector area was 2.5 cm².

The cooling system was similar to that described in Ref. 8. Cold nitrogen gas entered the Styrofoam box through horizontal slits near the top, and exited through a chimney tube that extended to 3 cm from the bottom of the cell chamber. The Styrofoam box was placed in a Plexiglass box (1-cm-thick walls), which in turn was surrounded by a sheet-brass Faraday cage. Three copper-Constantan thermocouples measured the temperature at the top and bottom of the cell and in the electrode area. A fourth thermocouple at the gas entry slits was connected to the temperature controller.

The amplifier (#8) was described in Ref. 11. The 0–97% response time of the circuit including the cell was 40 ns. The 1.7-MeV x-ray pulses were 30 or 100 ns in duration, delivering 3 or 10 × 10⁹ eV/g to the sample. Mobilities were measured with both positive and negative applied voltages to check for effects of adventitious fields.

C. Physical properties of the fluids

Densities of the liquid phase were obtained from Ref. 14. Those of the gas phase below 0.03 g/cm³ were calculated by means of the Beattie-Bridgeman equation.¹⁵ The vapor pressures needed were taken from Ref. 16. Densities above 0.03 g/cm³ were calculated from the equation of rectilinear diameters, the parameters of which were obtained from the densities of the liquids and low-density gases. The results agreed with those in Ref. 17. The critical temperature, pressure, and density of methane are $T_c = 191$ K, $P_c = 4.64$ MPa, $n_c = 6.1 \times 10^{21}$ molecule/cm³.^{14,17} The value for n_c used in Ref. 13 is too small by 21%, which causes a displacement of the results in Figure 1 of that reference.

III. RESULTS

A. Electric field effect

To facilitate comparison between data from the gas and liquid phases, all fields discussed herein were divided by the number density of the fluid. The standard unit is 1 Td = 1 × 10⁻¹⁷ V cm²/molecule, which is equivalent to 61 kV/cm in the critical fluid.

In the low-density gas the mobility is independent of field strength at $E/n \lesssim 0.010$ Td (Figure 1). Above this threshold the mobility increases. There is a slight increase of the threshold field at high densities, reaching 0.02–0.03 Td at the critical density (Fig. 1).

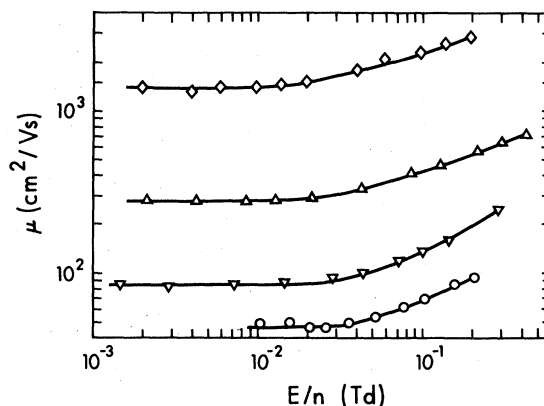


FIG. 1. Electron mobilities μ in gaseous methane at different densities, as functions of the density-normalized field strength E/n Td ($=10^{-17}$ V cm²/molecule). Densities and temperatures ($n/10^{21}$, T): \diamond , 0.16, 124; Δ , 0.73, 154; ∇ , 2.2, 178; \circ , 6.1, 193. Data were obtained in a "gas cell" with electrodes near the top. The lowest curve corresponds to a supercritical gas; the others represent vapors in equilibrium with the liquid. $T_c = 191$ K.

The field effect undergoes a change of sign in the liquid phase at $n \approx 8 \times 10^{21}$ molecule/cm³ $\approx 1.3n_c$ (Fig. 2). The threshold field then reduces with increasing density, reaching 0.013 Td at the density of the mobility maximum and remaining there at higher densities (Fig. 2).

In the low-density gas the field effect becomes noticeable when the electron drift velocity $v_d \approx 270$ m/s (Fig. 3). The threshold drift velocity increases with density, reaching ~ 1000 m/s in the critical fluid. Further increase of density into the liquid range causes a rapid increase in

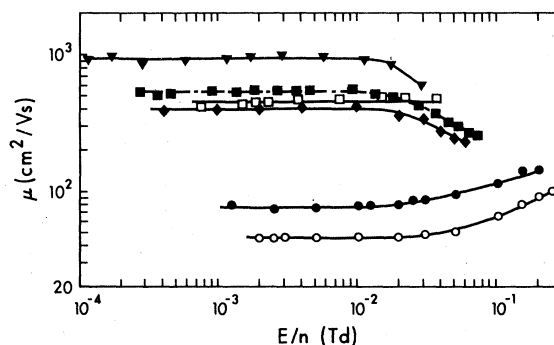


FIG. 2. Electron mobilities μ in liquid and supercritical methane, plotted against the density-normalized electric field strength E/n . Densities and temperatures ($n/10^{21}$, T): \blacksquare , 17.0 molecule/cm³, 91 K; \blacklozenge , 15.5, 122; \blacktriangledown , 10.7, 178; \square , 8.3, 189; \circ , 6.1, 193; \bullet , 6.1, 196. Data were obtained in a "liquid cell" with electrodes near the bottom.

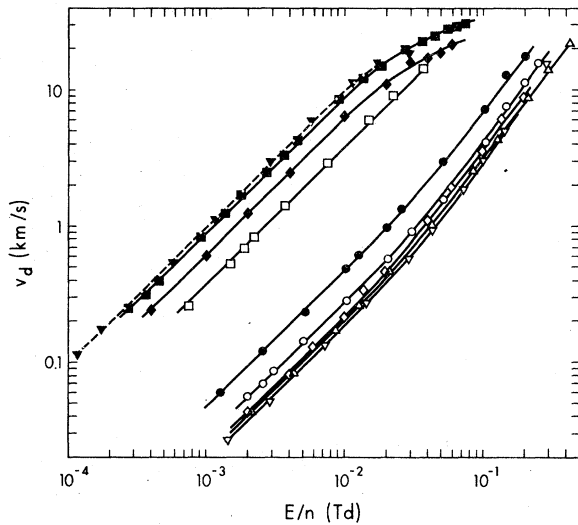


FIG. 3. Electron drift velocities v_d in liquid and gaseous methane, as functions of the density-normalized field strength E/n . Symbols as in Figs. 1 and 2.

the threshold drift velocity as the magnitude of the field effect decreases and ultimately changes sign. In the normal liquid the velocity threshold $v_d^{\text{thr}} \approx 10$ km/s (Fig. 3).

B. Temperature and density effects

An Arrhenius plot of the mobilities in the coexistent gas and liquid phases forms a loop (Fig. 4). Results of previous workers^{5,18,19} are included for comparison. Values for the liquid at $(10^3/T) > 7$ agree with $\pm 15\%$. The higher pressure used by Engles and Kimmenade shifted the mobility maximum to a higher temperature,⁵ but the number density at the maximum was $(1.07 \pm 0.03) \times 10^{22}$ molecule/cm³ in both cases (Fig. 5 and Ref. 5).

The linear portion of the curve for the gas phase in Fig. 4 has a slope that corresponds to the heat of vaporization of methane, 7.9 kJ/mol. This indicates that the mobility is inversely proportional to the coexistence vapor density at $T < 140$ K.

A plot of the density-normalized mobility μn against n in the coexistent fluids contains a shallow minimum at $n \approx 0.3n_c$ in the gas phase and another in the liquid at $n \approx 2.2n_c$ (Fig. 5). However, if the gas is kept at a constant temperature, say $T = T_c + 3 = 194$ K, the gas-phase minimum disappears. The value of μn is then constant up to $n \approx 0.5n_c$ and increases at higher densities (Fig. 5). The analogous liquid-phase measurements, varying the density at constant temperature, could not be made with the present apparatus.

In the supercritical gas the mobility increases

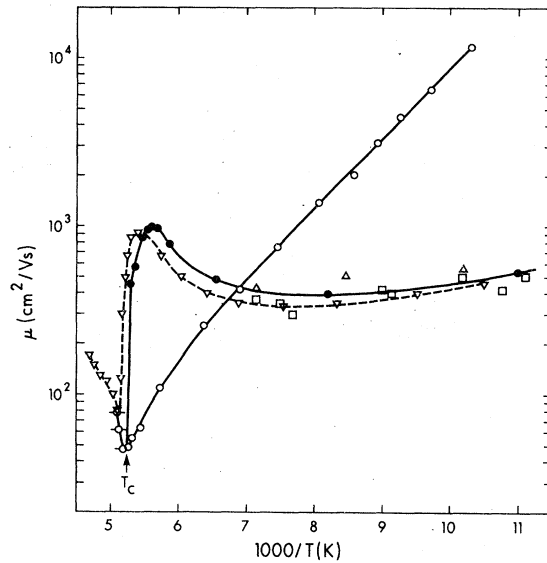


FIG. 4. Arrhenius plot of thermal-electron mobilities (low-field-strength limits) in the coexistent liquid (●) and gas (○) phases. Values in the superheated gas at the critical density are indicated by ○. Results from Ref. 5 (▽, 5.1 MPa), 18 (□), and 19 (△) are included for comparison.

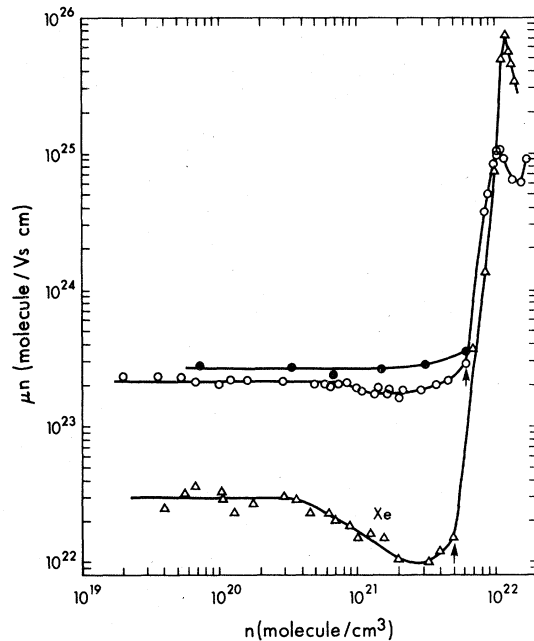


FIG. 5. Plot of μn (low-field-strength limit) against n for thermal electrons in the coexistent liquid and gas phases of methane (○) and xenon (△, Ref. 11). The arrows mark n_c . Some of the methane points are averages of two sets of results at the same density; ● represents methane at $T_c + 3 = 194$ K.

with temperature at either constant density or constant pressure (Fig. 4).

The temperature coefficient of mobility in the gas at constant density increases at an accelerating rate with density (Fig. 6). In the low-density gas the mobility varies as $T^{0.45}$, which is equivalent to an apparent activation energy of 0.6 kJ/mol. At the critical density near T_c the strong temperature dependence is equivalent to an activation energy of ~ 40 kJ/mol. The results are summarized in Table I.

Since the mobility increases upon increasing either the temperature or the field strength, one might expect that increasing the sample temperature would decrease the field dependence. Furthermore, increasing the field strength should decrease the temperature dependence of the mobility. Both expectations are fulfilled (Fig. 7).

The values of μn obtained at 297 K were about 20% higher than those calculated from earlier reports for $n = 10^{17} - 10^{19}$ molecules/cm³ and $T = 296 \pm 4$ K (Fig. 7).

IV. DISCUSSION

A. Field effect

1. Low-density gas

The mobility in methane at $n < 6 \times 10^{20}$ molecule/cm³ (< 22 amagat) in the coexistence vapor is field dependent at $E/n > 0.012$ Td (Figs. 1 and 8). The threshold field in the low-density gas increases somewhat with temperature. For example, at 297 K and $n = 7.1 \times 10^{19}$ molecule/cm³ the threshold is 0.025 ± 0.005 Td (Fig. 7). In previous studies of low-density methane, at 296 ± 4 K, mobilities were estimated at $E/n \geq 0.05$ Td,²⁰⁻²³ so the electrons were always somewhat epithermal. The increase of mobility with field strength is visible in the earlier plots at the lowest fields.²⁰⁻²³

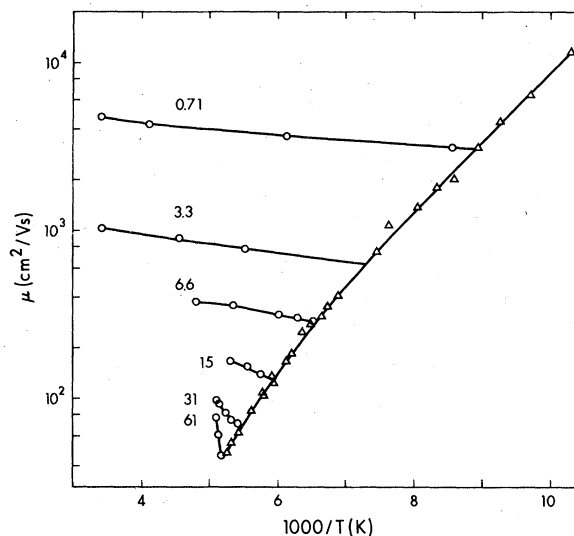


FIG. 6. Arrhenius plot of thermal-electron mobilities (low-field-strength limits) in methane gas at different densities (O). The numbers labeling the lines are the densities in units of 10^{20} molecule/cm³. Mobilities in the gas along the vapor-liquid coexistence curve are represented by Δ . The line through the data for 7.1×10^{19} molecule/cm³ was calculated from Eq. 9 by means of the cross sections in Fig. 11.

Duncan and Walker²⁴ measured the ratio of the diffusion coefficient to the mobility, D/μ , in the low-density gas at ~ 291 K. They found the electrons to be still slightly epithermal at the lowest-magnitude field used, $D/\mu = 1.2kT/e$ at 0.025 Td, although the plot of D/μ against E/n had become flat. The small discrepancies between their results and ours may be attributed to uncertainties in both sets of experiments.

Elastic scattering of electrons by individual molecules in the gas is kinetically equivalent to

TABLE I. Temperature coefficients of thermal-electron mobilities in methane gas at different densities.

Density		T range (K)	E_μ^a (kJ/mol)	$-\Delta H^b$ (kJ/mol)	$-\Delta S^b$ (J/mol K)	S(0) ^c	$-\Delta S^b/S(0)$
$(10^{20}$ molecule/cm ³)	n/n_c						
0.71	0.012	117-297	0.6			1.0	
3.3	0.049	135-295	1.1			1.1	
6.6	0.108	153-208	1.5	3.2	27	1.4	19
15.0	0.24	170-187	3.7	7.1	43	2.3	19
31	0.51	185-196	9.0	22	117	6	20
61	1.00	192-196 ^d	40	100	493	29	17

^a From Fig. 6.

^b From Eq. 18.

^c From Eq. 5, at the average temperature in the range.

^d $T_c = 191$ K.

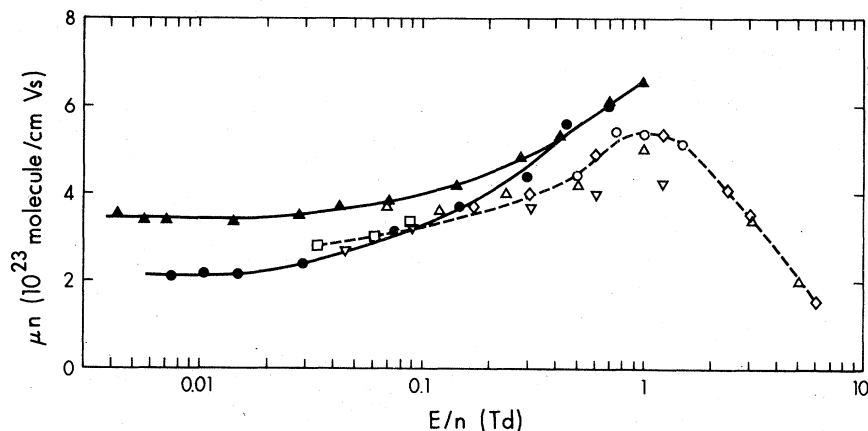


FIG. 7. Density-normalized mobilities as functions of E/n at different temperatures: \blacktriangle represents $n = 7.1 \times 10^{19}$ molecule/cm³, $T = 297$ K; \bullet , $n = 6.8 \times 10^{19}$, $T = 112$. Earlier results are shown for comparison: ∇ , $n = 10^{18}$ – 10^{19} , $T = 298$ K, Ref. 20; Δ , $n = 10^{17}$ – 10^{18} , $T \approx 293$? K, Ref. 21a; \circ , $n = 10^{17}$ – 10^{18} , $T = 300$ K, Ref. 21b; \diamond , $n = 10^{17}$ – 10^{18} , $T = 293$ K, Ref. 22; \square , n not given ($\approx 10^{19}$?), $T = 298$ K, Ref. 23.

scattering by phonons.²⁵⁻²⁸ The effective mass M^* of a phonon is given by $M^*c_0^2 = kT$, where c_0 is the velocity of low-frequency sound. In the low-density gas $c_0 = (\gamma kT/M)^{0.5}$, where γ is the heat-capacity ratio and M is the molecular mass.^{17c} One therefore obtains $M^* = M/\gamma \approx 0.75M$ in low-density methane.^{17b} Furthermore, when elastic scattering is the dominant process that moderates the electron energy, the electron drift velocity should become nonlinear with field strength when the drift velocity $v_d \approx c_0$.²⁷ The velocity of sound is therefore a useful parameter in assessing electron scattering processes even in the single-scatterer regime.

The velocity of low-frequency sound in saturated methane vapor at $n = 2 \times 10^{19}$ – 1×10^{21} molecule/cm³ is $c_0 = 280 \pm 10$ m/s.¹⁷ In these vapors the electron drift velocity becomes superlinear with field strength, that is, electron heating becomes noticeable, at $v_d^{\text{thr}} = 270 \pm 30$ m/s (Figs. 3 and 8).

Thus $v_d^{\text{thr}}/c_0 = 1.0 \pm 0.1$ in low-density methane gas (Fig. 9), which implies that the electrons lose energy mainly through elastic collisions under these conditions.

The value of the ratio v_d^{thr}/c_0 in other gases increases with decreasing sphericity of the molecules. The values determined to date are: xenon,¹¹ 0.7; methane, 1.0; neopentane,²⁹ 5; cyclopentane,³⁰ 11; cyclohexane,³⁰ 14; isopentane,²⁹ 15; and n pentane, >100 .²⁹ A larger value of the ratio indicates a larger contribution of inelastic collisions to thermal-electron transport in the gas. The relative importance of inelastic collisions therefore increases as the alkane molecules become less spherelike.

2. Density effect

The values of μn and the threshold of the field effect are constant at $n < 6 \times 10^{20}$ molecules/cm³ (Figs. 5 and 8), indicating that each electron in-

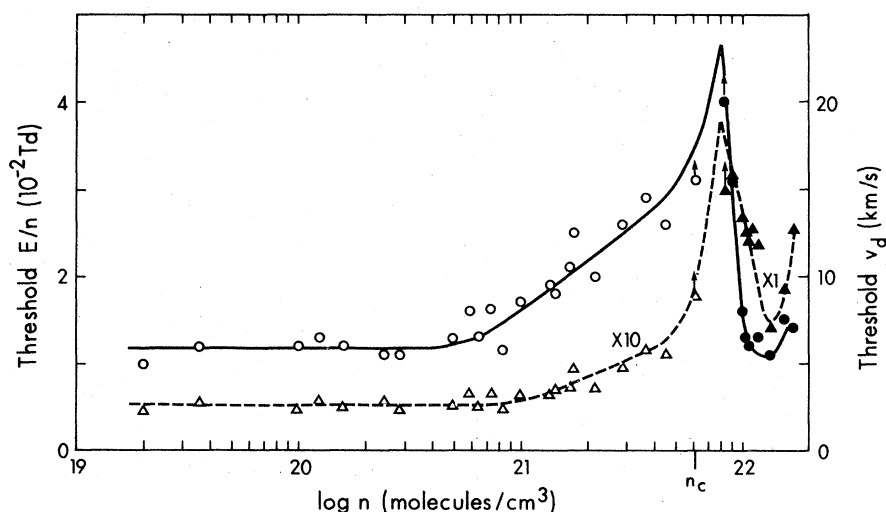


FIG. 8. Threshold electric field strength (\circ , gas; \bullet , liquid) and threshold electron drift velocity (Δ , $10v_d$, gas; \blacktriangle , v_d , liquid) above which electron heating occurs, plotted against the coexistence fluid density. For \circ , $d\mu/dE$ is positive; for \bullet , $d\mu/dE$ is negative. The thresholds at the critical density n_c were measured at $T_c + 2$ K and are lower limits for the values at T_c . The thresholds in the liquid at $n = 8.3 \times 10^{21}$ are also lower limits.

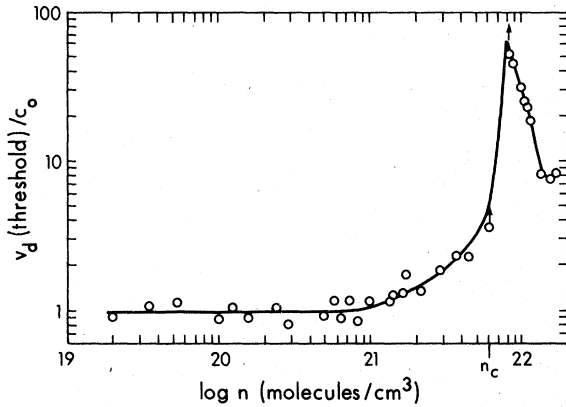


FIG. 9. Ratio of threshold drift velocity for electron heating to the speed of low-frequency sound, v_d^{thr}/c_0 , plotted against the density of the coexistence fluids.

teracts with one molecule at a time. At $n > 6 \times 10^{20}$, μn decreases (Fig. 5) and the threshold field increases (Fig. 8). These changes are due to enhanced scattering by multibody interactions. The effect differs from the density-enhanced scattering described by Atrazhev and Iakubov¹² for helium, hydrogen, and nitrogen, which would be observed only when the scattering is dominated by the short-range repulsive interaction. In such systems the Ramsauer-Townsend effect does not occur. In methane, as in xenon, scattering at low densities is dominated by the long-range polarization (attractive) interaction and the Ramsauer-Townsend effect is prominent.^{10,11} In such systems the multibody effects discussed by Atrazhev and Iakubov would cause the mobility to increase ("attenuation of the interaction"¹²), and this effect dominates the enhanced scattering at $n > 3 \times 10^{21}$ (Fig. 5). The decrease in mobility observed in the coexistence vapor at $n > 6 \times 10^{20}$ molecule/cm³ in methane, or $n > 4 \times 10^{20}$ in xenon, is attributed to quasilocalization of the electron by Van der Waals clusters of molecules. The clusters may be considered as density fluctuations:



Quasilocalization is an inelastic process, which causes an increase of the threshold field. This process will be discussed further in Sec. IV B.

At $n > 6 \times 10^{21}$ molecules/cm³ there is a rapid increase in μn (Fig. 5) and in the threshold field (Fig. 8). The sign of $d\mu/dE$ reverses at $n \approx 8 \times 10^{21}$. During the sign change the threshold field increases to a cusp, then reduces rapidly to a

value similar to that in the low-density gas (Fig. 8).

The similarity in the threshold fields at the highest and lowest densities is consistent with the single-scatterer approximation in the Cohen-Lekner model of electron transport^{27,28} in liquids made up of spherelike molecules.

The field effect at densities $6 \times 10^{20} < n < 8 \times 10^{21}$ contains contributions from both the Ramsauer-Townsend effect and quasilocalization. The contributions of these processes are shifted in opposite directions by changing the temperature (see Sec. IV C).

A plot of the threshold drift velocity against the density of the coexistence fluids is similar in shape to that of the threshold field (Fig. 8). However, at densities above the cusp the threshold drift velocity does not return to a value similar to that in the low-density gas, but to a value about 40 times higher. This difference is consistent with the model of Cohen and Lekner,^{27,28} which works quite well for quasifree electrons in simple liquids near the triple point.^{31,32} It involves the assumption that the scattering cross section of the molecules is reduced by the long-wavelength limit of the structure factor $S(0)$ so the electron mobility at high densities, μ_{hd} , is increased by the inverse of this factor.

$$\mu_{\text{hd}} = \mu_{\text{ld}}/S(0), \quad (4)$$

where μ_{ld} is the mobility in the low-density gas, for which $S(0) = 1$, and³³

$$S(0) = nkT\chi_T, \quad (5)$$

where χ_T is the isothermal compressibility of the fluid. According to this model one might expect the threshold drift velocity in the high-density liquid to be given by

$$v_d^{\text{thr}}{}_{\text{hd}} = v_d^{\text{thr}}{}_{\text{ld}}/S(0)_{\text{hd}}. \quad (6)$$

In liquid methane at 95 K, with $n = 1.67 \times 10^{22}$, one has $S(0) = 0.033$.³⁴ The 30-fold increase in threshold drift velocity predicted by this model accounts for most of the observed 40-fold increase (Fig. 8). The value of $S(0)$ increases with temperature, which explains the slope of the extreme right end of the threshold v_d curve in Fig. 8. It does not explain the minimum at 1.3×10^{22} molecule/cm³ nor the maximum at 8×10^{21} molecule/cm³. This behavior can be explained qualitatively by a screening effect and the passing through zero of the molecular scattering length at a certain density, similar to that proposed for argon.³⁵ On the high-density side of the scattering minimum the scattering length is positive, and the cross-section-versus-energy curve no longer possesses a minimum at low energies. One may then say

that the Ramsauer-Townsend minimum no longer exists, or some may prefer to say that the Ramsauer-Townsend minimum has moved to a negative energy. This conclusion is supported by the change of sign of the field dependence of the mobility in the low-density liquids of methane (Fig. 2) and xenon.¹¹ However, quantitative aspects of the model remain a problem.³²

Electron transport seems to be moderately well understood in low-density methane gas^{24,36} and in the liquid near the triple point, but not at intermediate densities.

In liquid methane near its triple point the ratio of the threshold drift velocity to the speed of sound equals 8 (Fig. 9). The values of the ratio in the liquids argon, krypton, and xenon near their triple points, where inelastic scattering is negligible, are approximately unity.³¹ Krypton is the noble element that has physical properties (polarizability, Van der Waals radius, critical temperature) most similar to those of methane. In krypton near its triple point $v_d^{\text{thr}}/c_0 \approx 0.8$.³¹ The ratio is tenfold larger in methane than in krypton, which indicates that inelastic collisions make an important contribution to moderating the electron energy, even at energies < 0.1 eV, in liquid methane. The total elastic plus inelastic scattering is also greater in methane than in krypton, since thermal-electron mobilities in the liquids near the triple points are 540 and ≥ 1800 cm²/Vs, respectively.

The ratio v_d^{thr}/c_0 equals 1.0 at $n < 1 \times 10^{21}$ and 8 at $n > 13 \times 10^{21}$ (Fig. 9). At intermediate densities the ratio rises to a cusp ≥ 60 at $n = 8 \times 10^{21}$; the cusp occurs in the liquid under its vapor pressure at one degree below T_c . Although the increase of the ratio at intermediate densities probably contains a contribution from inelastic processes, the cusp is due simply to the change of sign of $d\mu/dE$. Near the cusp, electron heating becomes appreciable at a field strength lower than that indicated by v_d^{thr} . The heating is not detected because increasing the electron energy ϵ has little effect on μ in this region: $d\mu/d\epsilon \approx 0$.

B. Temperature effect

1. Low-density gas

The electron scattering cross section of methane molecules varies with electron energy. The variation at low energies is obtained from the temperature dependence of the mobility at low field strengths (Fig. 6). Using the notation of Phelps,³⁷ we may represent the momentum-transfer cross section σ_v as a power series in v , the relative velocity of the electron with respect to the molecule:

$$\sigma_v^{-1} = \sum_j b_j v^{1-j}, \quad (7)$$

where b_j is an empirically determined constant. Equation 7 is based on the assumption that the density-normalized mean time between collisions, τn , can be represented by a power series:

$$\tau n = (\sigma_v v)^{-1} = \sum_j b_j v^{-j}, \quad (8)$$

where n is the number of molecule/cm³. For a Maxwellian distribution of velocities, the density-normalized mobility μn is given by

$$\mu n = \sum_j B_j (2kT/m)^{-j/2}, \quad (9)$$

where $B_j = (e/m)b_j(\frac{3}{2} - \frac{1}{2}j)!/(\frac{3}{2})!$, e and m are the electron charge (1.6×10^{-12} when μ is in cm²/Vs) and mass, respectively, and $(\frac{3}{2})! \equiv \Gamma(\frac{5}{2})$. The values of j and B_j are obtained by fitting experimental values of μn at different temperatures to Eq. (9). The collision cross section is then obtained from (10).

$$\sigma_v^{-1} = \frac{m}{e} \sum_j \frac{(\frac{3}{2})!}{(\frac{3}{2} - \frac{1}{2}j)!} B_j v^{1-j}. \quad (10)$$

When the electron energy is only varied over a small range, as in changing the gas temperature by a factor of two, a single term in (7) or (9) is often adequate. One then has $\mu n \propto T^{-j/2}$, and j is simply determined from the slope of a plot of $\log \mu n$ against $\log T$. This procedure has been used in many studies³⁸ and an equivalent formulation to the above is given elsewhere.³⁰ The common practice^{20,37} of using two terms in (7) or (9), while restricting the values of j to integers, does not offer an obvious advantage.

The mobilities at 7.1×10^{19} molecule/cm³ (Fig. 6) gave $j = -0.9$, while those at 3.3×10^{20} molecule/cm³ gave $j = -1.1$. The apparent value of j becomes acceleratingly more negative as n increases, owing to multibody interactions. The low-density limit is $j = -0.9$. The early work of Bowman and Gordon²⁰ indicated $j \approx -3$; this might have influenced subsequent estimates of the variation of σ_v at electron energies $\epsilon < 0.06$ eV.^{22,24} However, the results of the early temperature study²⁰ were quite scattered (Fig. 10), so the value of j derived from them is uncertain.

The values of σ_v estimated from the present work are shown in Fig. 11. The cross sections derived earlier^{10,20,22,24} are dependable at $\epsilon > 0.1$ eV, but not at lower energies. For example, the lowest field strength used by Pollock was 0.17 Td,²² whereas the field-effect threshold at 293 K would have been at 0.02–0.03 Td (Fig. 7). Bowman and Gordon assumed the threshold to lie at

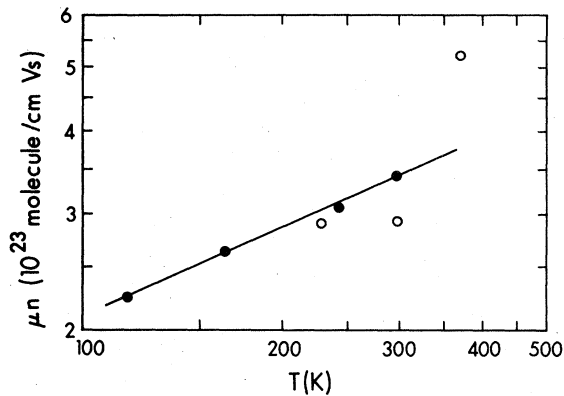


FIG. 10. Effect of temperature on the low-field values of μn at the low-density limit: ● represents the present work, $n = 7.1 \times 10^{19}$; ○, Ref. 20, $n = 0.7 \times 10^{19}$ molecule/cm³.

0.9 Td.²⁰ The most reliable values of σ_v are represented by the solid line in Fig. 11. Experimentally, $1-j$ represents the average slope of a plot of $\log \sigma_v$ against $\log v$ taken over the relevant range of v .

The Maxwellian distribution curve for 200 K in Fig. 11 indicates the approximate energy range that affects the transport of thermal electrons. Mobilities were measured at temperatures from 117 to 297 K, so the relevant energy range is ~ 0.002 to 0.2 eV. In this region one has

$$\sigma_v = 0.0142v^{-1.9} \text{ cm}^2. \quad (11)$$

Taking an average cross section equivalent to one assumed to be independent of v , one obtains

the following for a Maxwellian distribution of velocities.³⁹

$$\sigma_{av} = \langle v \rangle / \langle v / \sigma_v \rangle \quad (12)$$

$$= (m/2kT)^{(1-j)/2} / b_j \Gamma(\frac{3}{2} - \frac{1}{2}j). \quad (13)$$

For methane at 300 K, $\sigma_{av} = 4.0 \times 10^{-16} \text{ cm}^2$.

The above conclusions have been substantiated by using many different forms of σ_v in place of Eq. (7) and the appropriate integral equation for μn in place of (9). The integration was done numerically over 29 steps of $\log v$. The best fit of the mobilities at $n = 7.13 \times 10^{19}$ molecule/cm³ and $117 \leq T \leq 297$ K was provided by the full curve in Fig. 11 at $0.001 \leq \epsilon \leq 0.3$ eV. The cross sections reported in Refs. 20, 22, and 24 generated temperature coefficients much larger than that observed experimentally.

2. Density effect

At gas densities $> 3 \times 10^{20}$ molecule/cm³ the temperature coefficient of mobility increases superlinearly with density (Fig. 6 and Table I). In the same density region the mobility μ^0 of quasifree electrons increases.⁴⁰ Taking the low field ($E/n = 0.06$ Td) mobilities at 293 K⁴⁰ as a measure of μ^0 , the value of the ratio of $(\mu^0)_n$ at density n to the low-density limit $(\mu^0)_{ld}$ is $(\mu^0)_n / (\mu^0)_{ld} = 1.05$ at $n = 3 \times 10^{20}$, 1.25 at $n = 11 \times 10^{20}$ and extrapolates to 3 ± 1 at $n_c = 61 \times 10^{20}$ molecule/cm³. The density-normalized mobility for any values of T and n is

$$\mu n = (\mu^0)_n f, \quad (14)$$

where f is the fraction of electrons in the quasi-

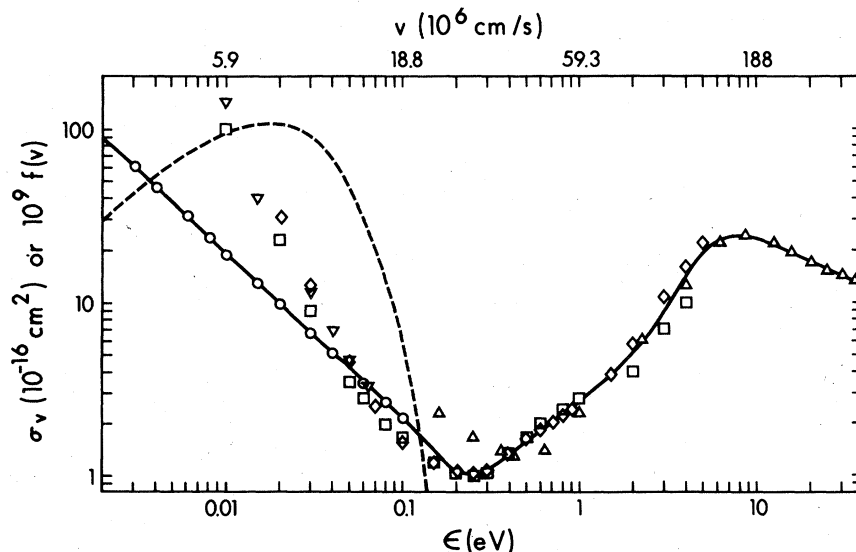


FIG. 11. Momentum-transfer cross section σ_v of low-density methane gas as a function of electron energy ϵ and velocity v : ○ represents the present work; ▽, Ref. 20; ◇, Ref. 22; □, Ref. 24; △, the total cross section, Ref. 10a. Here — represents the favored values of σ_v and - - - represents $f(v) = N^{-1} dN/dv$ for a Maxwellian distribution of electrons at 200 K, where $f(v)dv$ represents the fraction of electrons that have velocities between v and $v+dv$.

free state.

In the dense gas, where each molecule is within interaction distance of at least one other, the dynamic equilibria (1) and (2) reduce to density fluctuations in the fluid. A fluctuation of sufficient magnitude is a possible localization site for an electron, so one may write^{41,42}



It follows that

$$\begin{aligned} f &= [e_{\text{qt}}^-] / ([e_{\text{qt}}^-] + [e_{\text{loc}}^-]) \\ &= (1 + [\text{site}]K)^{-1} \end{aligned} \quad (17)$$

and

$$(\mu^0 n)_n / \mu n - 1 = e^{\Delta S'/R} e^{-\Delta H'/RT}, \quad (18)$$

where $[e_{\text{qt}}^-]$, $[e_{\text{loc}}^-]$, and $[\text{site}]$ represent the concentrations of those species,

$$\begin{aligned} K_{16} &= e^{\Delta S_{16}^0/R} e^{-\Delta H_{16}^0/RT}, \\ [\text{site}] &= e^{\Delta S_{15}^0/R} e^{-\Delta H_{15}^0/RT}, \end{aligned}$$

$$\Delta S' = \Delta S_{15}^0 + \Delta S_{16}^0 \approx \Delta S_{15}^0, \quad \Delta H' = \Delta H_{15}^0 + \Delta H_{16}^0.$$

The density fluctuations, and thus the $[\text{site}]$, are largest in the coexistence vapor. They diminish as the gas is heated at constant density.

The large temperature coefficient at the critical density a few degrees above T_c , 40 kJ/mol (Table I), is attributed mainly to the reverse of (15) rather than to the reverse of (16). The energy of localization of the electron depends partly on the magnitude of the density fluctuation in a zone commensurate with the zero-point value of λ of the electron. Considering that there is a distribution of fluctuation magnitudes $\partial n / \partial V$ and that a localization energy of kT is sufficient to produce the observed 2–3 fold reduction in mobility, the average localization energy is taken to be $-\Delta H_{16}^0 = \Delta H_{-16}^0 \approx kT \approx 2$ kJ/mol. The remaining 38 kJ/mol in the near-critical gas is attributed to $-\Delta H_{15}^0$. Thus $\Delta H' \approx \Delta H_{15}^0$.

Values of $(\mu^0 n)_n$ at a given n and T were estimated by using the 0.71 curve in Fig. 6 to obtain $(\mu^0 n)_{\text{id}}$, and multiplying it by $(\mu^0 n)_n / (\mu^0 n)_{\text{id}}$ obtained from the data of Lehning,⁴⁰ using interpolation or extrapolation where necessary. Plots of $\log[(\mu^0 n)_n / \mu n - 1]$ against T^{-1} gave the values of $\Delta S'$ and $\Delta H'$ listed in Table I. At each density one has $\Delta H' \approx T\Delta S'$, or $\Delta G' \approx \Delta G_{15}^0 \approx 0$, as expected for a vapor near the coexistence region.

The observed value of $\Delta S'$ is approximately proportional to the structure factor $S(0)$, with $\Delta S'/S(0) \approx -19$ J/mol K (Table I). The value of $S(0)$ is related to the magnitude of the density fluctuations,⁴³ and electron localization serves as a probe for fluctuations of a certain magnitude. As a comparison with the above value of -19 J/mol K, the entropy of condensation of methane at its normal boiling point is -80 J/mol K and its magnitude reduces to zero at the critical point.

The Lekner model for electron transport in critical fluids⁴⁴ predicted an excessive dependence on $S(0)$ because it implied too great a value for ΔH_{-16} .

C. Threshold field

Heating the low-density vapor increased the threshold field slightly (Fig. 7). This is attributed to the larger average energy of the electrons and the consequent larger amount of energy exchanged per collision in the warmer gas. Heating the gas at the critical density decreased the threshold field somewhat (Fig. 2), owing to the reduction in extent of quasilocalization and of the attending inelastic processes.

The field effect associated with quasilocalization always contributes a positive term to $d\mu/dE$. Heating the electrons decreases the probability of quasilocalization and thereby increases μ . On the other hand the scattering-cross-section curve shown in Fig. 11 shifts to lower energies with increasing density, owing to destructive interference of the long-range polarization interactions. This means that $d\sigma_v/dv$ generates a positive contribution to $d\mu/dE$ in low-density methane ($j < 0$), but a negative contribution at high densities ($j > 0$). The observed $d\mu/dE$ changes sign when the negative contribution from $d\sigma_v/dv$ is great enough to cancel the positive contribution from quasilocalization. This occurs at $n \approx 8 \times 10^{21}$ (Fig. 8). The value of j probably changes sign at $n \approx 7 \times 10^{21}$ molecule/cm³. Raising the temperature at constant n (in a pressure vessel) would ultimately remove the quasilocalization contribution and cause $d\mu/dE$ and j to change sign at the same density.

ACKNOWLEDGMENTS

We would like to thank the staff of the Radiation Research Center for help with the electronics, and B. V. Paranjape for assistance with the wording of Sec. IVA 1.

- ¹H. Schnyders, S. A. Rice, and L. Meyer, *Phys. Rev.* **150**, 127 (1966).
- ²J. A. Jahnke, L. Meyer, and S. A. Rice, *Phys. Rev. A* **3**, 734 (1971).
- ³T. Kimura and G. R. Freeman, *Can. J. Phys.* **52**, 2220 (1974).
- ⁴J.-P. Dodelet and G. R. Freeman, *J. Chem. Phys.* **65**, 3376 (1976).
- ⁵J. M. L. Engels and A. J. M. van Kimmenade, *Chem. Phys. Lett.* **48**, 451 (1977).
- ⁶J.-P. Dodelet and G. R. Freeman, *Can. J. Chem.* **55**, 2264 (1977).
- ⁷N. E. Cipollini and A. O. Allen, *J. Chem. Phys.* **67**, 131 (1977).
- ⁸J.-P. Dodelet and G. R. Freeman, *Can. J. Chem.* **55**, 2893 (1977).
- ⁹P. G. Fucchi and G. R. Freeman, *J. Chem. Phys.* **56**, 2333 (1972).
- ¹⁰(a) C. Ramsauer and R. Kollath, *Ann. Phys. (Leipzig)* **4**, 91 (1930); (b) **3**, 536 (1929).
- ¹¹S. S.-S. Huang and G. R. Freeman, *J. Chem. Phys.* **68**, 1355 (1978).
- ¹²V. M. Atrazhev and I. T. Iakubov, *J. Phys. D* **10**, 2155 (1977).
- ¹³N. E. Cipollini, R. A. Holroyd, and M. Nishikawa, *J. Chem. Phys.* **67**, 4646 (1977).
- ¹⁴(a) R. W. Gallant, *Physical Properties of Hydrocarbons* (Gulf, Houston, Tex., 1968), Vol. 1; (b) V. Jansoone, H. Gielen, J. de Boelpaep, and O. B. Verbeke, *Physica* **46**, 213 (1970).
- ¹⁵J. O. Hirschfelder, C. F. Curtiss, and R. B. Bird, *Molecular Theory of Gases and Liquids* (Wiley, New York, 1954).
- ¹⁶*Handbook of Chemistry and Physics*, 49th ed., edited by R. C. Weast (Chemical Rubber Co., Cleveland, Ohio, 1968).
- ¹⁷(a) R. D. Goodwin, *The Thermophysical Properties of Methane from 90 to 500 K at Pressures to 700 Bar*, Natl. Bur. Stand. Tech. Note 653 (U.S. GPO, Washington, D.C., 1974); (b) S. Angus, B. Armstrong, and K. M. de Reuck, *International Thermodynamic Tables on the Fluid State—5: Methane*, International Union of Pure and Applied Chemistry Chemical Data Series No. 16 (Pergamon, Oxford, 1978); (c) E. Hausmann and E. P. Slack, *Physics* (Van Nostrand, New York, 1944), p. 412.
- ¹⁸G. Bakale and W. F. Schmidt, *Z. Naturforsch. Teil A* **28**, 511 (1973).
- ¹⁹M. G. Robinson and G. R. Freeman, *Can. J. Chem.* **52**, 440 (1974).
- ²⁰C. R. Bowman and D. E. Gordon, *J. Chem. Phys.* **46**, 1878 (1967).
- ²¹(a) E. B. Wagner, F. J. Davis, and G. S. Hurst, *J. Chem. Phys.* **47**, 3138 (1967); (b) D. R. Nelson and F. J. Davis, *J. Chem. Phys.* **51**, 232 (1969).
- ²²W. J. Pollock, *Trans. Faraday Soc.* **64**, 2919 (1968).
- ²³L. G. Christophorou, R. P. Blaustein, and D. Pittman, *Chem. Phys. Lett.* **18**, 509 (1973).
- ²⁴C. W. Duncan and I. C. Walker, *J. Chem. Soc. Faraday Trans. 2* **68**, 1514 (1972).
- ²⁵F. B. Pidduck, *Proc. London Math. Soc.* **15**, 89 (1916).
- ²⁶B. Davydov, *Phys. Z. Sowjetunion*, **8**, 59 (1935); **12**, 269 (1937).
- ²⁷W. Shockley, *Bell Syst. Tech. J.* **30**, 990 (1951), see pp. 1018–24.
- ²⁸M. H. Cohen and J. Lekner, *Phys. Rev.* **158**, 305 (1967).
- ²⁹I. György and G. R. Freeman, *J. Chem. Phys.* **70**, 4769 (1979).
- ³⁰S. S.-S. Huang and G. R. Freeman, *Can. J. Chem.* **56**, 2388 (1978).
- ³¹L. S. Miller, S. Howe, and W. E. Spear, *Phys. Rev.* **166**, 871 (1968).
- ³²J. A. Jahnke, N. A. W. Holzwarth, and S. A. Rice, *Phys. Rev. A* **5**, 463 (1972).
- ³³D. L. Goodstein, *States of Matter* (Prentice-Hall, Englewood Cliffs, 1975), Chap. 4.
- ³⁴Ref. 17(a), p. 118; $\chi_T = [(MOL/L)(DP/DD)]^{-1}$; $S(0) = 0.082T/(DP/DD)$.
- ³⁵J. Lekner, *Phys. Lett. A* **27**, 341 (1968).
- ³⁶P. Kleban and H. T. Davis, *Phys. Rev. Lett.* **39**, 456 (1977).
- ³⁷J. P. Pack and A. V. Phelps, *Phys. Rev.* **121**, 798 (1961).
- ³⁸L. G. Christophorou, *Atomic and Molecular Radiation Physics* (Wiley-Interscience, London, 1971), Secs. 4.3 and 4.4.
- ³⁹L. G. H. Huxley and R. W. Crompton, *The Diffusion and Drift of Electrons in Gases* (Wiley, New York, 1974), Chap. 3.
- ⁴⁰H. Lehning, *Phys. Lett. A* **29**, 719 (1969).
- ⁴¹P. W. Anderson, *Phys. Rev.* **102**, 1008 (1958).
- ⁴²J. Jortner and A. Gaathon, *Can. J. Chem.* **55**, 1801 (1977).
- ⁴³D. L. Goodstein, *States of Matter* (Prentice-Hall, Englewood Cliffs, 1975), Chaps. 1 and 4.
- ⁴⁴J. Lekner and A. R. Bishop, *Philos. Mag.* **27**, 297 (1973).